Optimizing Phylogenetic Eigenvector Regression: Union Eigenvectors, Robust Estimation, and Flexible Application to Comparative Analyses

Zheng-Lin Chen and Deng-Ke Niu*

MOE Key Laboratory for Biodiversity Science and Ecological Engineering, College of Life Sciences, Beijing Normal University, Beijing, 100875, China

*Correspondence author: Deng-Ke Niu, College of Life Sciences, Beijing Normal University, Beijing, 100875, China.

E-mail addresses: chenzljx@gmail.com (Z.-L. Chen), dkniu@bnu.edu.cn, dengkeniu@hotmail.com (D.-K. Niu)

Abstract

Phylogenetic eigenvector regression (PVR) is widely used in ecology and evolution because it represents phylogenetic structure through modular eigenvectors rather than model-specific assumptions. Despite this flexibility, its implementation faces two challenges: the choice of eigenvectors and the default use of least-squares regression, which may reduce robustness under non-stationary evolution. A further source of uncertainty concerns the applicability of conventional rules for model complexity, such as the "samples-per-variable (SPV) ≥ 10" guideline. Here we propose an optimized PVR framework that addresses these issues. First, we show that eigenvectors selected independently from different traits often diverge, leading to inconsistent results, and that using their union provides stronger control of phylogenetic non-independence. Second, we evaluate robust regression estimators within PVR, demonstrating that PVR-MM, and in some cases even PVR-L2, maintain high accuracy under non-stationary evolutionary shifts where other non-robust methods deteriorate. Third, through simulation we reassess the SPV ≥ 10 rule, showing that PVR tolerates eigenvector counts well beyond this conventional threshold, offering more flexibility but requiring careful monitoring. Extensive simulations across diverse tree structures and evolutionary scenarios confirm that the optimized framework enhances both accuracy and robustness. By clarifying best practices for eigenvector selection, regression estimation, and model complexity, our results provide practical guidelines that improve the reliability of PVR and broaden its utility for phylogenetic comparative analyses.

KEYWORDS: phylogenetic comparative methods; phylogenetic eigenvector regression (PVR); robust regression; evolutionary shift; phylogenetic autocorrelation; phylogenetic signal; trait correlation.

1. Introduction

Comparative studies of traits across species must account for phylogenetic non-independence (Cornwallis and Griffin, 2024; Dewar et al., 2025; Felsenstein, 1985; Garamszegi, 2014). Among the available approaches, phylogenetic eigenvector regression (PVR) has become widely used in ecology and evolutionary biology because it expresses phylogenetic information as separable and modular eigenvectors (EVs) (Diniz-Filho et al., 2012a; Diniz-Filho et al., 2014; Diniz-Filho et al., 2011; Diniz-Filho et al., 1998; Diniz-Filho and Tôrres, 2002). This representation not only provides flexibility beyond predefined evolutionary models, but also allows integration with other sources of autocorrelation (e.g., spatial or temporal) (Kühn et al., 2009; Maynard et al., 2022; Peres-Neto et al., 2012; Safi and Pettorelli, 2010; Wang et al., 2019) and with machine learning methods (Debastiani et al., 2021; Penone et al., 2014). Such versatility helps explain the broad adoption of PVR in ecological applications, and underscores the importance of refining its implementation (Divíšek et al., 2018; Gao et al., 2023; Lanuza et al., 2023; LeRoy et al., 2020).

Despite its utility, two issues limit PVR performance. First, EVs selected from each trait separately may yield inconsistent results, raising concerns when analyzing relationships between traits. Second, conventional PVR relies on ordinary least squares regression, which can be sensitive to non-stationary evolutionary shifts or outliers. These challenges motivate the development of optimized strategies that improve reliability while retaining the flexibility of PVR.

Here, we propose an optimized PVR framework that combines (i) a union-based EV set (*EV_U*) to capture shared phylogenetic structure, (ii) robust regression estimators to reduce sensitivity to non-stationarity (Adams et al., 2024; Huber, 1964; Slater and Pennell, 2014; Yu and Yao, 2017), and (iii) a reassessment of the conventional "samples-per-variable (SPV, i.e., events per variable) ≥ 10" rule (Babyak, 2004), showing that PVR remains reliable with far fewer samples per predictor and emphasizing the need to check EV counts before model fitting. Using extensive simulations under a range of evolutionary scenarios and tree structures, we assess the accuracy of these strategies relative to established comparative methods, and highlight the conditions under which optimized PVR offers particular advantages.

2. Materials and methods

2.1. Simulation of phylogenetic trees

We evaluated PVR on five fully bifurcating trees—chosen to vary branch-length scaling, taxon sampling, and topological balance—generated with *stree* (**ape** 5.8) and, where necessary, combined with *paste.tree* (**phytools** 2.3-0) (Paradis and Schliep, 2019; Revell, 2024):

1. **Baseline**: 128-tip balanced tree, Grafen (1989) scaling $\rho = 1$.
2. **Compressed deep branches**: 128-tip balanced tree, $\rho = 0.1$ (short ancestral, long terminal branches).
3. **Elongated deep branches**: 128-tip balanced tree, $\rho = 2$ (long ancestral, short terminal branches).
4. **Extreme imbalance**: 128-tip ladder (comb-shaped) tree, $\rho = 1$.
5. **Sparse sampling**: 16-tip balanced tree, $\rho = 1$.

2.2. Simulated trait generation

We generated paired traits X_1 and X_2 on each of the five phylogenetic trees under six evolutionary settings adapted from Revell (2010), Adams et al. (2024), and Chen et al. (2025). In all cases, $X_2 = \beta X_1 + \varepsilon$, where β controls the underlying association (default $\beta = 1$), ε contributes random variance. In the two shift scenarios (items 5–6 below) a separate parameter s displaces trait means on a single deep branch. The same eight magnitudes (10□□, 0.01, 1, 4, 16, 64, 256, and 1024) served either as the variance d of $\mathcal{N}(0, d)$ for non-shift cases or as the shift size s. Brownian-motion (BM) traits were simulated with *rTraitCont* (**ape** 5.8, rate = 1, hence variance = 1), and normal values with *rnorm* (**stats** 4.1.3). Each magnitude was replicated 1 000 times, yielding 8 000 datasets per scenario and 48 000 per tree. The six scenarios for X_1 and X_2 are:

1. **BM1 & BM1+BM2**: X_1 and ε each follow an independent BM, their linear combination $X_2 = \beta X_1 + \varepsilon$ remains a process of Brownian type.
2. **BM & BM+Norm**: X_1 under BM; ε follows independent and identically distributed (i.i.d.) normal, diluting phylogenetic signal in X_2.
3. **Norm & Norm+BM**: X_1 follows i.i.d. normal; ε under BM , giving X_2 some phylogenetic structure.
4. **Norm1 & Norm1+Norm2**: Both traits follows i.i.d. normal (no intended phylogenetic signal).
5. **X_1-only shift**: an abrupt shift of magnitude s is applied only to X_1 on a deep branch. Otherwise, $\beta = 1$, X_1 follows BM with variance = 1, and ε is i.i.d. with $\mathcal{N}(0, 0.01)$.

6. **Dual-trait shift**: The same shift s is applied simultaneously to X_1 and ε; elsewhere both traits evolve independently under BM, with $\beta = 0$.

These settings span a broad range of phylogenetic signals, noise intensities, stationary versus non-stationary dynamics, and single- versus dual-trait shift scenarios for benchmarking PVR variants and comparator methods. For implementation details of the shift simulations, see Chen et al. (2025)

2.3. Correlation benchmark and accuracy metric

For every simulation we saved trait values at all nodes, then calculated standardized changes on each branch, $\Delta X_1/L$ and $\Delta X_2/L$, where L denotes the branch length. This branch-wise differencing is inspired by Felsenstein's (1985) phylogenetically independent contrast (PIC) in its aim to isolate independent evolutionary changes, but here the node values are already known, so no ancestral-state reconstruction or BM assumption is required. Because branches are independent, these change vectors form a tree-wide "ground-truth" sample.

We measured the association between $\Delta X_1/L$ and $\Delta X_2/L$ with Spearman's rank correlation (robust to non-normality and outliers). The procedure detects both causal links ($\beta \neq 0$) and incidental correlations that arise when two independent traits happen to drift in parallel (Chen et al., 2025).

A comparative method was counted as correct for a dataset when both the direction and statistical significance ($p < 0.05$ or not) it inferred matched the benchmark Spearman result; otherwise it was incorrect. For each scenario-noise/shift level-tree combination, 1 000 replicate datasets were generated. The accuracy of a method is the fraction of correct outcomes across the 1 000 replicates for that experimental combination.

2.3. Phylogenetic eigenvectors selection methods

EVs were obtained by principal-coordinate analysis of the double-centred cophenetic distance matrix, yielding $n - 1$ axes. For each trait (X_1 or X_2) we selected a subset of EVs with three published criteria (Diniz-Filho et al., 2012a; Diniz-Filho and Nabout, 2009):

1. **ESRRV**: keep EVs whose Pearson or Spearman correlation with the focal trait is significant, choosing the test according to the trait's normality.

2. **mAIC**: forward stepwise regression adding EVs that lower Akaike Information Criterion (AIC), implemented with *stepAIC()* (**MASS** 7.3-55) (Venables and Ripley, 2002).
3. **mMorI**: forward selection until the residual Moran's I is minimised. Because phylogenetic autocorrelation is almost always positive, we modified this rule to stop as soon as residual Moran's I becomes negative; if it never does, selection continues to the usual non-significant threshold.

Custom R wrappers *ESRRV()* and *MoransI()* implement rules 1 and 3, while all other calculations use the original **PVR** package (Diniz-Filho et al., 2012a; Diniz-Filho et al., 1998; Diniz-Filho et al., 2012b).

2.4. Correcting phylogenetic autocorrelation in trait regressions

After EV selection we compared four ways to purge phylogenetic signal:

1. ***EV_X*$_1$ model**: $X_1 \sim X_2 + EV_X_1$ — covariates are the EVs chosen for X_1.
2. ***EV_X*$_2$ model**: $X_2 \sim X_1 + EV_X_1$ — uses the EVs chosen for X_2. Writing it in reverse form, $X_1 \sim X_2 + EV_X_1$, controls the same EVs, so the correlation (and its *p*-value) is identical, although the regression slope becomes the reciprocal of the original.
3. ***EV_U* model**: $X_2 \sim X_1 + EV_U$ — *EV_U* is the union of EVs selected from both traits.
4. **Residual correlation**: Regress each trait on its own EVs, then take the Pearson correlation of the residuals. To curb type-I error from over-fitting, *p*-values were based on $df = n - k - 1$, where n is the number of species and k the number of EVs in *EV_U*. While this conservative adjustment may reduce power, it controls for inflated false positives due to shared structure among eigenvectors (Diniz-Filho and Tôrres, 2002).

2.5. Robust regressions in PVR

To test the sensitivity of PVR to outliers and non-normal errors we compared its with five different regression estimators:

1. **L2**: as termed in robust regression (Huber, 1964), corresponds to the standard OLS estimator that minimizes squared residuals under homoscedastic normal errors. It was implemented using *lm()* (package **stats**, R 4.1.3).
2. **L1**: least-absolute-deviation (*lad()*, **L1pack** 0.41-245) (Phillips, 2002).

3. **M**: Huber-type M-estimator (*rlm()*, **MASS** 7.3-55) (Venables and Ripley, 2002).
4. **S**: high-breakdown S-estimator (*lmRob()*, **robust** 0.7-4) (Gervini and Yohai, 2002).
5. **MM**: S start followed by an M step (*lmRob()*, **robust**).

Among these estimators, L2 serves as the baseline; L1, M, S, and MM offer progressively stronger resistance to leverage points while retaining efficiency. For detailed properties and phylogenetic applications of these estimators, see Adams et al. (2024).

3. Results

Unless otherwise noted, in the subsequent analyses, PVR regressions control phylogeny by including as covariates the eigenvectors selected for each trait separately (EV_X_1, EV_X_2) or their union (*EV_U*).

3.1. Eigenvector selection and budgeting

3.1.1. Variation in EV counts across selection rules and tree topologies

We applied three EV-selection rules (ESRRV, mAIC, mMorI) separately to X_1 and X_2; the resulting EV sets, together with their union (*EV_U*), were carried forward as candidate covariates for examination. As detailed later through mathematical derivations and PVR accuracy assessments (Section 3.3), *EV_U* plays an important role in controlling phylogenetic autocorrelation, so here we give special attention to |*EV_U*| when comparing outcomes across rules, without disregarding the other EV sets.

Across all four tree scenarios with 128 species, the size of the *EV_U* set differed markedly among selection rules (Fig. 1). mAIC consistently returned the largest sets, with medians ranging from 123 to 125 EVs across topologies. By comparison, ESRRV produced *EV_U* medians ranging from 6 to 31, and mMorI from 1 to 37; under the balanced 128-species tree, both methods returned a median of 9. Replications at $n = 16$ (Fig. S1) reproduced the same qualitative pattern as observed at $n = 128$, indicating that EV counts are determined primarily by tree topology and the selection rule rather than by sample size.

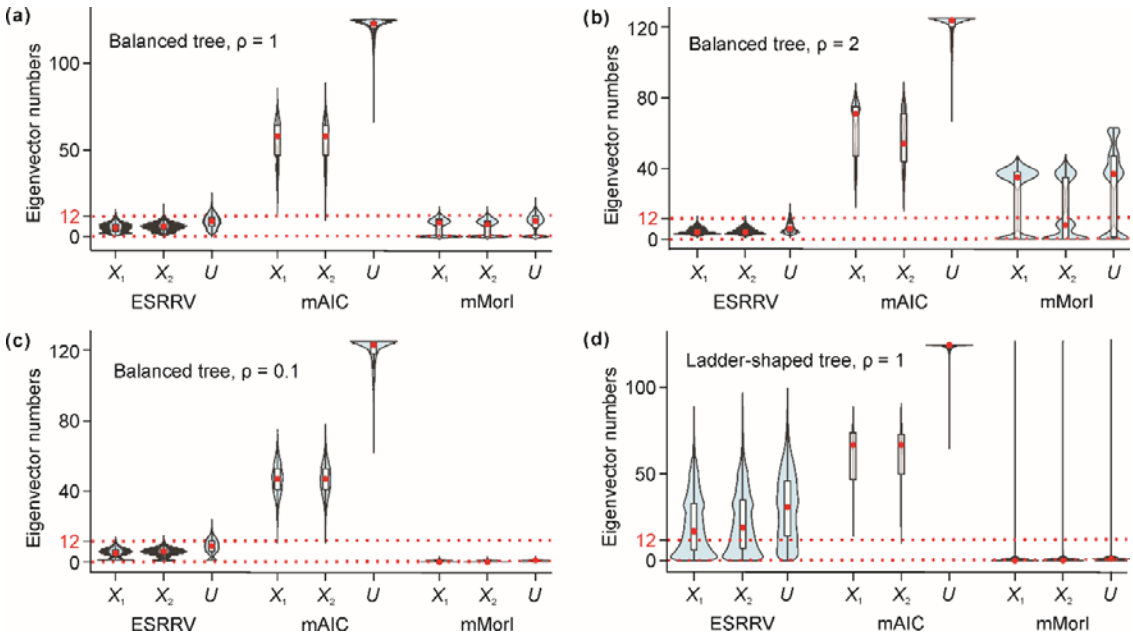

Fig. 1. Eigenvectors retained by three selection criteria (ESRRV, mAIC and mMorI) for a 128-species phylogenetic tree. EVs were picked separately for X_1 and X_2; *EV_U* is their union. Violin outlines depict the full distribution of selected eigenvector counts; white boxes show the inter-quartile range, black whiskers the 5th–95th percentiles, and red dots mark the median of each distribution. The red dashed line marks the ~13□predictor upper bound implied by the conventional samples□per□variable ≥ 10 guideline, calculated here assuming one non□EV predictor. Selection criteria are described in Materials and Methods.

3.1.2. Reassessing the SPV ≥ 10 Rule in PVR

In our SPV calculations, both retained EVs and non-EV predictors are counted, so the number of parameters is |EV| + $p_{\text{non□EV}}$ (with one biological predictor, |EV| + 1). The "SPV ≥ 10" rule, widely recommended to avoid over-parameterization and unstable inference in conventional regression (Austin et al., 2017; Babyak, 2004; Peduzzi et al., 1996), suggests that the ratio of species per (|EV| + 1) should should be at least 10. However, unlike biological or environmental predictors, however, EVs are orthogonal components derived from the phylogenetic distance matrix, so this rule does not have the same interpretation in PVR as in ecological regressions.

To test this idea, we conducted simulations on balanced trees with ρ = 1 and n = 128 species, using six evolutionary scenarios. For each scenario, we examined five |*EV_U*| settings, corresponding to species-per-(|*EV_U*| + 1) ratios of approximately 1.5, 2, 3, 6, and the EV count selected by mMorI. In this setting, mMorI typically returned fewer EVs than the conventional SPV ≥ 10 threshold yet was already sufficient to control phylogenetic autocorrelation and avoid false positives due to residual structure. We then augmented the

mMorI-selected *EV_U* set by adding eigenvectors in descending eigenvalue order to reach the 6, 3, 2, and 1.5 ratio targets ($|EV_U| \approx 20$, 42, 63, and 84, respectively), allowing us to isolate the impact of increased EV counts from that of phylogenetic independence control. When independence was effectively addressed, differences in PVR accuracy across these *EV_U*-count gradients are attributable mainly to potential overfitting from excessive predictors.

In the six simulation scenarios, the impact of EV count on PVR accuracy varied. In the three gradual-evolution cases (Figs.2a, 2b, and 2d), accuracy began to decline when $|EV_U| = 63$ and deteriorated substantially at $|EV_U| = 84$. In the Norm & Norm+BM and dual-trait shift scenarios (Figs. 2c and 2f), accuracy showed only slight variation across EV counts, and in both cases the mMorI-selected set (SPV ≥ 10) was not among the best performing. Under the single-shift condition (Fig. 2e), accuracy was identical across all EV counts, showing no sensitivity to EV number.

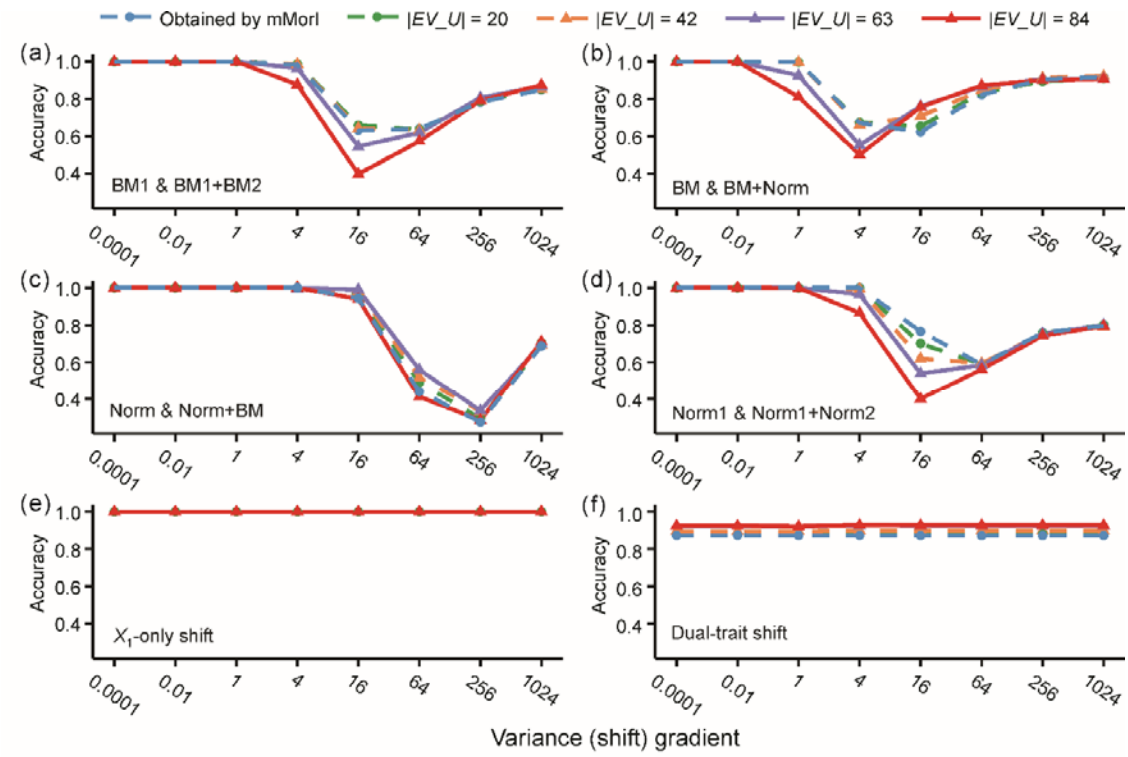

Fig. 2. Accuracy of PVR under six simulation scenarios with varying numbers of eigenvectors (EVs). Panels (a–d) show gradual-evolution settings and (e–f) shift scenarios, all simulated on a balanced phylogenetic tree with 128 species and uniformly scaled branch lengths ($\rho = 1$). Lines represent PVR accuracy when *EV_U* was fixed at 20, 42, 63, or 84, or determined by mMorI (median = 9 EVs). For details on EV selection, scenario and accuracy definitions, see Materials and Methods; the data used to plot this figure appear in Table S1.

Taken together, these results indicate that the conventional SPV ≥ 10 rule, originally derived for non-orthogonal predictors in conventional regression modeling, does not directly apply to EVs in PVR; the orthogonality weakens the link between predictor count and overfitting risk. Under gradual-evolution conditions, accuracy remained acceptable down to a species-per-(|EVU|+1) ratio of ~3 (≈42 EVs), but declined at lower ratios (≈2 and 1.5), indicating ~3 as a practical minimum threshold. These findings also clarify the implications for EV selection rules. Across all tree topologies (Fig. 1 and Fig. S1), mAIC consistently returned excessively large EV sets, rendering it unsuitable for PVR. ESRRV generally yielded moderate counts and thus can be applied across topologies, but mMorI returned very few or even zero EVs in some cases, failing to control phylogenetic autocorrelation. From a methodological perspective, however, mMorI has the advantage of explicitly minimising residual Moran's I—the most direct criterion for removing phylogenetic dependence. Accordingly, in balanced trees with $\rho = 1$ where ESRRV and mMorI return similar EV counts, our subsequent comparisons indicate that mMorI should be preferred.

3.2. Discrepancies Between Predictors in EV Selection

Although the above results show that retaining somewhat larger EV sets does not substantially compromise PVR accuracy, most empirical analyses nevertheless rely on the EVs selected for specific predictors. In practice, however, the sets chosen for different biological variables may not be identical, and such discrepancies could potentially propagate to the PVR results. To investigate this possibility, we conducted simulations on balanced trees with 128 species and uniformly scaled branches ($\rho = 1$), using paired predictors to quantify the consequences of divergent EV sets for PVR inference.

3.2.1. Impact of assigning "predictor" and "response" labels on eigenvector choice

In typical PVR applications, the covariate set is drawn only from the EVs selected for the dependent trait. The designation of the dependent and independent trait strongly affects which eigenvectors are retained. Across 8 000 simulations per scenario (Table 1), the two trait-specific selections disagreed in 76.4% of cases on average, with the dual-shift scenario showing the highest discordance.

Table 1. Frequency with which the EV sets chosen for X_1 and X_2 do not match.

Simulation scenarios	ESRRV	mMorI
BM1 & BM1+BM2	83.3%	84.1%
BM & BM+Norm	80.4%	81.4%
Norm & Norm+BM	86.3%	75.8%
Norm1 & Norm1+Norm2	86.0%	4.5%
X_1-only shift	91.0%	49.2%
Dual-trait shift	94.5%	100%

Values represent the percentage of inconsistent selections across 8,000 simulations per scenario. Methods (ESRRV and mMorI) and scenarios are detailed in Materials and Methods. The raw data underlying this summary appear in Table S2.

3.2.2. Divergent PVR results when the two traits supply different EV sets

To measure how much PVR results depend on which trait supplies the eigenvectors, we ran two competing regressions for every simulation replicate under each EV-selection method (ESRRV and mMorI): OLS ($X_1 \sim X_2 + EV_X_1$) and OLS ($X_2 \sim X_1 + EV_X_2$). Each regression was recoded 1 when it produced a significant positive correlation ($p < 0.05$, slope ≥ 0) and 0 otherwise. A pair was deemed discordant when the two recodes disagreed (1/0 or 0/1).

Across the six evolutionary scenarios in total, ≈13% of comparisons (12 257 pairs) were identified as discordant, with the discordance rate ranging from 0.13% to 30.7% (Table 2). The highest discordance occurred in the dual-trait shift scenario (30.7% with ESRRV). Strikingly, even this 30.7% mismatch in the dual-trait shift scenario was not flagged as significant by McNemar's test. A closer look revealed that among the discordant comparisons, roughly half were "significant only in the EV_X_1 model" and half "significant only in the EV_X_2 model," producing an almost perfectly balanced 1/0 versus 0/1 table. This symmetry cancels out in McNemar's statistic, even though the two models disagree on nearly one-third of the samples.

Table 2. Proportion of simulations in which PVR models using the EV set from X_1 versus that from X_2 yield discordant results.

Simulation scenarios	ESRRV	mMorI

BM1 & BM1+BM2	19.8% ns	11.4% ns
BM & BM+Norm	9.18% ***	18.2% ***
Norm & Norm+BM	11.5% ***	10.8% ***
Norm1 & Norm1+Norm2	6.44% ns	0.13% ns
X_1-only shift	14.1% ***	6.02% ***
Dual-trait shift	30.7% ns	14.9% ***

Divergence is counted when the two regressions differ in statistical significance ($p < 0.05$ vs ≥ 0.05) or slope sign (≥ 0 vs < 0). Percentages are based on 8 000 datasets per scenario. McNemar's χ^2 test was run in R 4.3.1 with *exact2x2* (function *mcnemar.exact*, v1.6-9); Significance code: *** $p < 0.001$; ns $p > 0.05$. See Materials and Methods for details on EV selection methods (ESRRV and mMorI) and simulation scenarios. The raw data underlying this summary appear in Table S3.

3.2.3. Divergence in correlation coefficients due to EV set differences

To quantify how strongly the estimated trait association can shift when the eigenvector set is switched, we analysed the 12 257 discordant model pairs identified in § 3.2.2. For every discordant pair we computed

$$|\Delta\rho| = |pcor(X_1, X_2 + EV_X_1) - pcor(X_2, X_1 + EV_X_2)|.$$

73% simulations showed $|\Delta\rho| > 0.1$ and 15 % exceeded the more stringent $|\Delta\rho| > 0.5$ threshold, indicating that the choice of EV set alters not just significance but also the magnitude of inferred trait associations. Divergences were especially large in the X_1-only shift scenario: the median $|\Delta\rho|$ reached 1.04 with ESRRV and 0.97 with mMorI), implying that the two models usually assigned opposite signs to the correlation—a full reversal of biological interpretation (Fig. 3).

Beyond the 12 257 discordant comparisons, a further 73 318 model pairs used different eigenvector sets ($EV_X_1 \neq EV_X_2$) yet reached the same decision on significance and slope sign. Even within this ostensibly "stable" subset, effect sizes diverged appreciably: 31% of pairs showed $|\Delta\rho| > 0.1$ and 4% exceeded the stricter $|\Delta\rho| > 0.5$ threshold. The X_1-only shift scenario did not display a higher mean $|\Delta\rho|$ than the other scenarios, but it had the broadest spread (Fig. S2), indicating that large swings in effect size can still arise when only one trait experiences a phylogenetic shift.

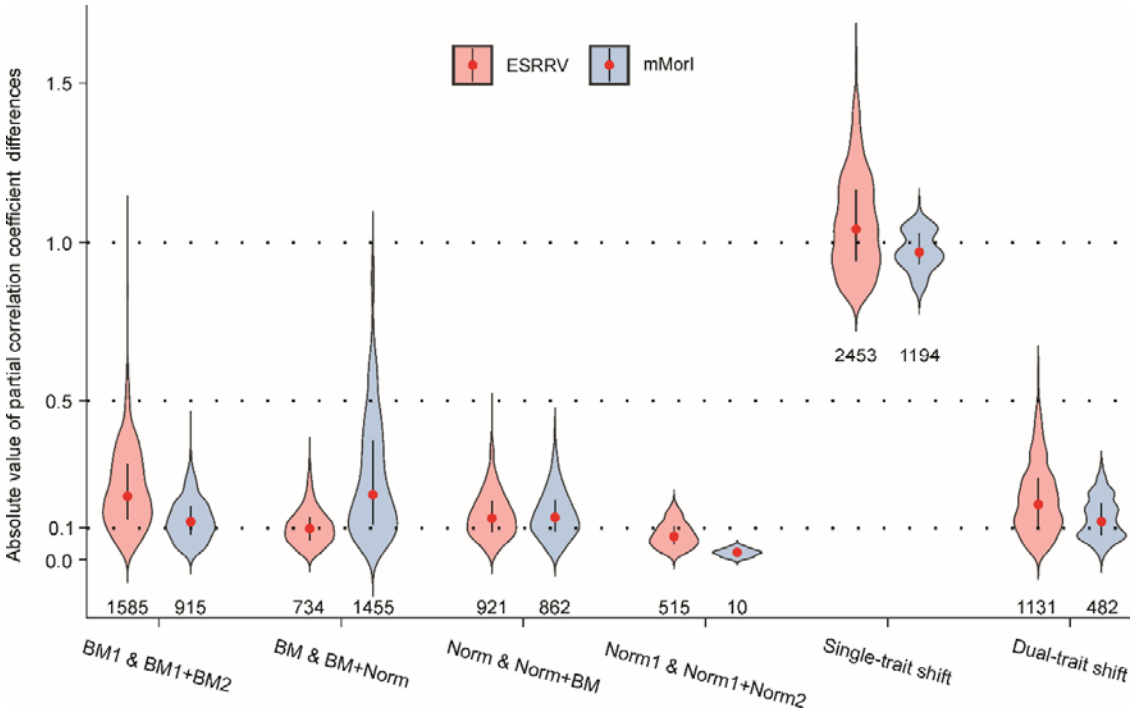

Fig. 3. Distributions of absolute differences in partial correlation coefficients between comparing PVR models using EV_X_1 versus EV_X_2 as covariates under six evolutionary scenarios. The violin plot illustrates the absolute differences in partial correlation coefficients $|\text{pcor}(X_1, X_2 + EV_X_1) - \text{pcor}(X_2, X_1 + EV_X_2)|$ for cases with conflicting PVR results; numbers beneath each violin give the sample size (n). Partial correlations were computed with ppcor::pcor() (Pearson). Red dots indicate the median values, black vertical bars span the inter-quartile range, and black whiskers extend to the 5th–95th percentiles. Paired t-tests revealed significant differences in partial-correlation estimates between EV_X_1 and EV_X_2 in every scenario (all $p < 0.001$) except when mMorI was applied to the Norm1 & Norm1+Norm2 scenario data, where the test was non-significant ($n = 10$, $p = 0.373$). See Materials and Methods for details of the EV-selection procedures (ESRRV, mMorI) and the BM, Norm and Shift simulation variants; the raw values plotted here are provided in Table S4.

Altogether, our results show that the EVs selected for different traits can diverge to very different degrees, with some cases showing only modest discrepancies while others reveal substantial non-overlap. These EV differences can in turn propagate into PVR regressions, producing variation in both statistical significance and correlation coefficients; the severity of such effects also varies across evolutionary scenarios, ranging from negligible shifts to large divergences, including sign reversals. While our analyses here focused on balanced trees with 128 species and $\rho = 1$, the patterns shown in Fig. 1b and Fig. 1d indicate that under alternative topologies—such as $\rho = 2$ balanced trees with mMorI, or ladder-shaped trees with ESRRV—the discrepancies between trait-specific EV sets are even greater, and the resulting distortions in PVR outcomes can be expected to be more severe.

3.3. Why Use the Union of Eigenvectors?

3.3.1. Theoretical Rationale for Using the Union of Trait-Specific EVs

PVR models built with EV_X_1 versus EV_X_2 —each selected independently for a single trait—often diverge in significance and coefficients. This inconsistency prompts a more fundamental theoretical question: can such per-trait EV sets fully control phylogeny when two traits share only part of their phylogenetic signal?

When either trait is filtered through only its own eigenvector set, phylogenetic structure unique to the partner trait remains unmodelled, biasing estimates. Our derivation (Text S1) shows that taking the union of both sets (*EV_U*) captures the full *P* component of Cheverud's (1985) $T = P + S$ framework, yielding more stable and unbiased regression results. This mirrors Westoby et al.'s (2023) critique that PGLS corrects phylogeny in the response but not in the predictor.

Motivated by the same concern, we will also examine a two-step alternative: first regress each trait on its own EVs to remove trait-specific phylogeny, and then fit an OLS regression to the resulting residuals to quantify the trait–trait association.

3.3.2. Performance of eigenvector selection methods and regression approaches

Building on the earlier results (Fig. 1a), where both ESRRV and mMorI produced admissible EV counts under a balanced tree with 128 species and uniformly scaled branches ($\rho = 1$), we next used simulations to assess whether the choice of selection method materially influences PVR outcomes. Our central focus, however, is to test whether regressions based on the union set *EV_U* outperform those relying on trait-specific EVs or residual approaches.

Fig. 4 compares eight PVR configurations—two EV-selection methods (ESRRV, mMorI), each combined with four regression strategies (EV_X_1, EV_X_2, *EV_U*, and residual). *EV_U* regressions (red lines)—regardless of whether paired with ESRRV (dashed) or mMorI (solid)—generally perform better than the other regression strategies (blue, green, and black lines) in most scenarios. Among these, mMorI + *EV_U* (red solid line) is consistently the top-ranked or co-top-ranked method across all six scenarios and shift magnitudes. This robustness makes it the most reliable configuration overall.

While residual-based regressions (black lines) also account for phylogenetic signals in both traits, their overall performance was generally inferior to that of *EV_U*-based strategies (Fig. 4). This discrepancy likely arises because removing phylogenetic signal separately for each trait can also eliminate shared components that carry true associations. In contrast,

EV_U integrates information from both traits within a single model, thereby preserving shared structure while controlling for phylogenetic effects, and consequently achieved higher accuracy across scenarios.

A notable special case is observed in Fig. 4e, where the two traits are highly correlated except for a large, abrupt shift in X_1 on a deep branch, which introduces a localized deviation. Under these conditions, all configurations yield identical results—represented by the overlapping red solid line—except for the combinations involving EV_X_2 (i.e., ESRRV + EV_X_2 and mMorI + EV_X_2). As for the other converging methods—*EV_U*, EV_X_1, and residual regressions—their similarity in accuracy may result from capturing a common set of critical eigenvectors that effectively represent the phylogenetic signal associated with the shift in X_1.

Nevertheless, when both ESRRV and mMorI yield admissible EV counts, we retained mMorI as the default configuration, owing to its consistent superiority across the tested scenarios. When considered alongside with the results from Fig. 1 and Fig. 2, our findings suggest adopting mMorI under balanced trees with ρ = 1 and ρ = 2, while relying on ESRRV for ρ = 0.1 balanced trees and ρ = 1 ladder-shaped trees, where mMorI frequently fails to return sufficient EVs.

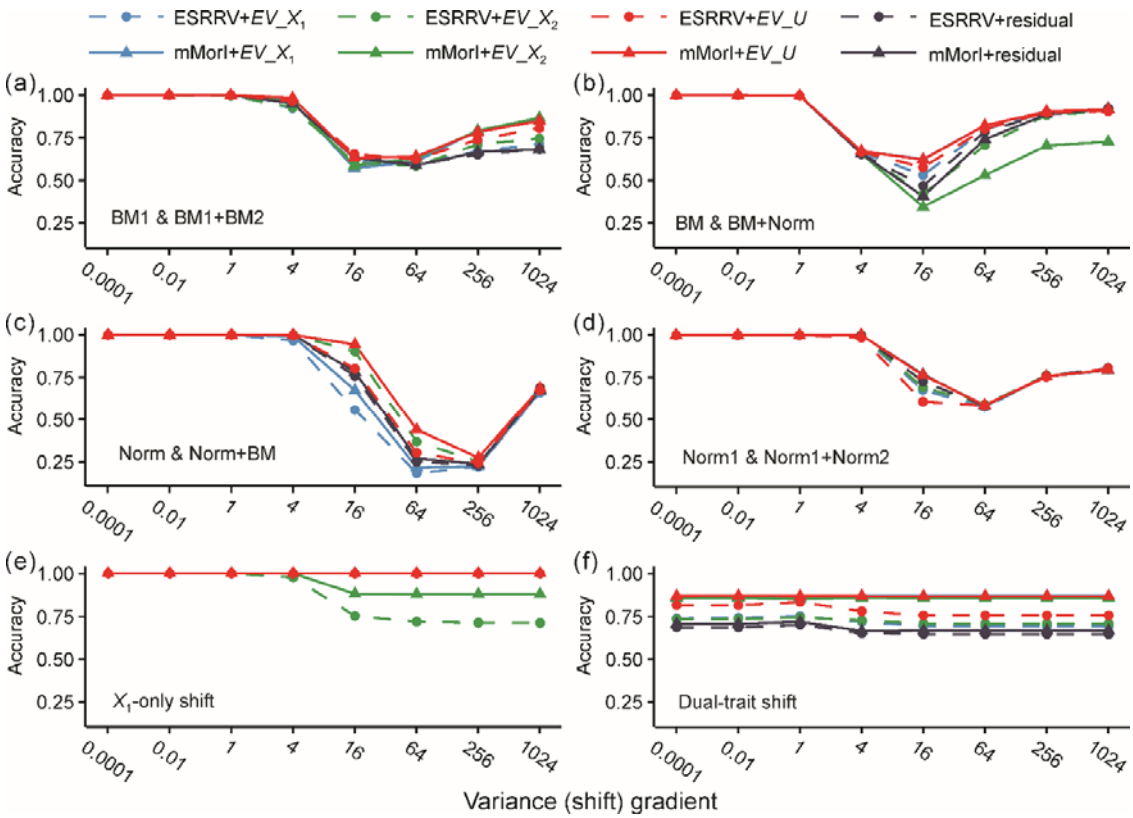

Fig. 4. Performance across different phylogenetic eigenvector (EV) selection methods and regression strategies. This figure compares two EV selection methods (ESRRV and mMorI), each combined with four regression approaches: (1) using EV_X_1 as covariates; (2) using EV_X_2; (3) using their union, *EV_U*; and (4) regressing the residuals of X_1 and X_2, each pre-adjusted by their respective EVs. Simulations were conducted on balanced trees with 128 species ($\rho = 1$), across six scenarios: (a) BM1 & BM1+BM2; (b) BM & BM+Norm; (c) Norm & Norm+BM; (d) Norm1 & Norm1+Norm2; (e) X_1-only shift; and (f) Dual-trait shift. In some cases, multiple method combinations produced identical results; their lines overlap and may appear as a single curve in the plot. For details on EV selection, scenario and accuracy definitions, see Materials and Methods. The source data for this figure are provided in Table S5.

3.4. EV_U-Based PVR as an Intrinsically Robust Framework

We evaluated five regression estimators—L1, L2, M, MM, and S—within the *EV_U*-based PVR framework. Here, PVR with the conventional least-squares estimator (L2) serves as the default implementation. Simulations were conducted using 128-species phylogenies under four topologies, with mMorI applied to 128-species balanced trees with $\rho = 1$ and $\rho = 2$, and ESRRV used for 128-species balanced trees with $\rho = 0.1$ and ladder-shaped trees with $\rho = 1$, as well as 16-species balanced trees with $\rho = 1$ analyzed under mMorI (Figs. S3–S7). Across these settings, L2, M, and MM yielded nearly identical accuracies in most scenarios, with their curves largely overlapping in the plots. Only in ladder-shaped trees under strong shift conditions did MM show a clear robustness advantage, while L2 and M remained indistinguishable or very close. Compared with these three estimators, the performance of L1 varied depending on the scenario; in contrast, S generally underperformed across multiple shift settings and was thus excluded from subsequent analyses. Estimator M was also omitted from later figures, as its outputs were nearly indistinguishable from L2 and were almost entirely overlapped in all scenarios, making its inclusion visually redundant.

Although the complete eigenvector set is determined solely by the tree's topology and branch lengths—independent of any trait—it already provides a rich basis for phylogenetically structured variation, spanning both gradual evolution and localized shifts. With appropriate selection, *EV_U* effectively captures this structure, leaving residuals close to i.i.d. normality. Under such conditions, the reweighting mechanisms of robust regression estimators like M and MM are scarcely activated (Huber, 1964). Consequently, the default L2 implementation of PVR performs essentially as robustly as M or MM, diminishing the need for specialized robust estimators in this framework. However, under extreme scenarios—such as ladder-shaped phylogenies combined with dual high-gradient trait

shifts—MM regression retains notable estimation stability, reflecting its inherent capacity to accommodate intense phylogenetic heterogeneity and noise.

3.5. Comparative Evaluation of Optimized PVR, PGLS, and PIC

To evaluate the performance of the optimized PVR approaches (implemented with L1, L2, and MM estimators), we used *EV_U* constructed from mMorI for 128-species balanced trees (ρ = 1, 2) and 16-species balanced trees (ρ = 1), and from ESRRV for 128-species balanced trees (ρ = 0.1) and ladder-shaped trees (ρ = 1). These approaches were compared against three established methods, PGLS, PIC-L2 (i.e., PIC-OLS), and PIC-MM (a robust variant recommended by Adams et al. (2024). For PGLS, the best-fitting evolutionary model was selected from five candidates—BM, Pagel's λ, Ornstein–Uhlenbeck (OU) with fixed α, OU with random α, and the Early-Burst (EB) model—using AIC, and is hereafter referred to as PGLS-optimal.

Across the phylogenetic structures described above, under the three gradual evolution settings (BM1 & BM1+BM2, Norm & Norm+BM, and Norm1 & Norm1+Norm2), the performance of the different PVR variants was generally lower than or at best comparable to that of PGLS-optimal and PIC-L2, and sometimes aligned with PIC-MM (Fig. 5 and Figs. S8–S11). In contrast, under the BM & BM+Norm condition, all methods except PGLS-optimal performed similarly, and they clearly outperformed PGLS-optimal.

In simulations with evolutionary shifts, regardless of whether the tree had 128 or 16 species, or whether the balanced trees were simulated with different values of ρ, PGLS-optimal and PIC-L2 consistently showed poor robustness (Figs. S8–S11). By contrast, PIC-MM and the PVR variants performed similarly and maintained strong robustness against increasing shift magnitudes. However, on ladder-shaped trees, the robustness of PVR-L1 and PVR-L2 deteriorated, with performance falling closer to that of PGLS-best and PIC-L2 (Fig. 5). In this setting, only the MM-based methods—PIC-MM and PVR-MM—were able to sustain high accuracy and effectively accommodate strong shifts.

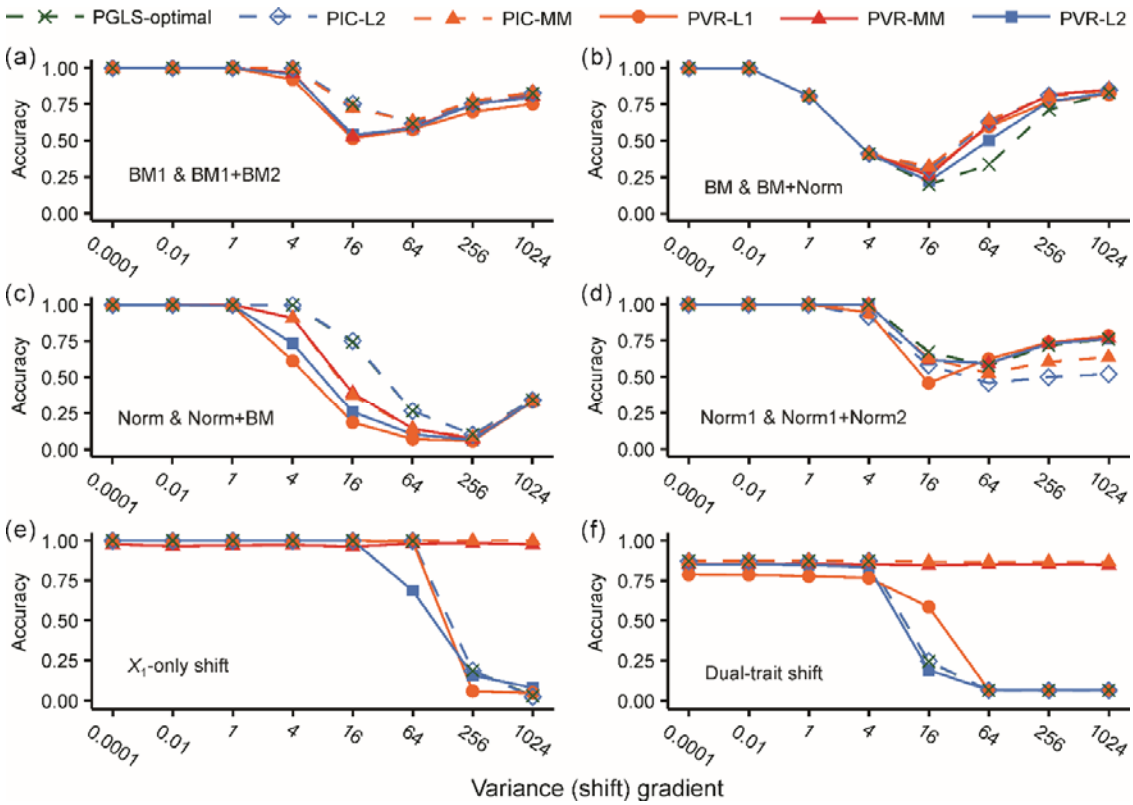

Fig. 5. Performance of PVR, PGLS, and PIC on 128-species ladder-shaped phylogenetic trees (ρ = 1). Comparisons were conducted under six evolutionary scenarios: (a) BM1 & BM1+BM2; (b) BM & BM+Norm; (c) Norm & Norm+BM; (d) Norm1 & Norm1+Norm2; (e) X_1-only shift; and (f) Dual-trait shift. All eigenvectors (EVs) were selected using the ESRRV criterion. For details on ESRRV, scenario definitions, and accuracy measures, see Materials and Methods. The data underlying this figure are provided in Table S6.

4. Discussion

PVR was originally proposed as a flexible method for modeling trait–trait correlations using phylogenetic eigenvectors (Diniz-Filho et al., 1998). While often viewed as less reliable than PGLS—due to its lack of explicit evolutionary modeling and inflated Type I error rates when using broken-stick criteria (Freckleton et al., 2011; Laurin, 2010; Pennell and Harmon, 2013)—PVR remains widely used in ecological research. Its strength lies in using separable and modular eigenvectors to represent phylogenetic structure, offering a model-agnostic and highly integrative design. This modularity allows easy incorporation into machine learning methods such as random forests and neural networks (Debastiani et al., 2021; Penone et al., 2014), supporting tasks like trait imputation and classification beyond regression. Moreover, because the eigenvectors are orthogonal, they can be jointly modeled with other sources of autocorrelation (e.g., spatial or temporal), a flexibility particularly

valuable in ecological settings where multiple forms of structure coexist (Kühn et al., 2009; Maynard et al., 2022; Safi and Pettorelli, 2010; Wang et al., 2019).

In this study, we revisit and optimize the PVR framework. We show that eigenvectors derived from different traits often diverge, and using their union (*EV_U*) more effectively controls phylogenetic non-independence. While our focus is on trait pairs, the logic extends to multi-trait settings, where incorporating all relevant trait-specific eigenvectors helps retain phylogenetic signal. However, care must be taken to avoid overfitting by limiting the number of retained eigenvectors.

Through the integration of robust estimators, we demonstrate that optimized PVR variants—especially PVR-MM and even PVR-L2—outperform PGLS and PIC under non-stationary evolutionary dynamics. This robustness likely stems from PVR's capacity to absorb localized, structured variation without assuming a specific evolutionary process (Diniz-Filho et al., 2015; Diniz-Filho et al., 2014; Diniz-Filho et al., 2019; Diniz-Filho et al., 2012b; Gouveia et al., 2013). Nonetheless, we acknowledge that under stationary conditions, traditional approaches like PGLS and PIC may remain more efficient. Our results thus challenge the long-standing view of PVR's inferiority, and underscore its potential as a robust and versatile phylogenetic method in non-equilibrium evolutionary contexts.

4.1. Dependence of PGLS performance on dependent variable selection

From Fig. 5 and Figs. S8–S11, PGLS-optimal performed worst in BM & BM+Norm, but achieved the best or near-best performance in the other three stationary conditions. In these more favorable scenarios, the dependent variable (X_2) exhibited stronger or comparable phylogenetic signal than the predictor (X_1), whereas in BM & BM+Norm, X_2 exhibited weaker signal.This pattern suggests that PGLS performance may be sensitive to the distribution of phylogenetic signal between variables, tending to perform best when the response variable carries the stronger signal. Preliminary analyses by Chen et al. (2023, preprint) suggest that signal imbalance can distort PGLS estimates, underscoring the importance of accounting for signal distribution in model selection. With an appropriate choice of response variable, PGLS may remain competitive—or even preferable—across all stationary conditions, including BM & BM+Norm.

4.2. Flexibility of eigenvector-based approaches in phylogenetic modeling

Unlike likelihood-based methods such as PGLS, which rely on predefined evolutionary models (Freckleton et al., 2011), PVR captures phylogenetic structure through eigenvector decomposition. This model-free design offers greater flexibility when evolutionary processes deviate from standard models (e.g., BM, OU, EB) or when model uncertainty is high (Diniz-Filho et al., 2014). Given the limited set of available models and the difficulty of reliably distinguishing among them, likelihood-based approaches remain inherently constrained.

PVR is also structurally advantageous when modeling correlations between traits. PGLS inherits from OLS the assumption that predictors are fixed and measured without error (Casson and Farmer, 2014; Jarantow et al., 2023; McArdle, 1988; Osborne and Waters, 2002), which may conflict with biological reasoning—especially when the predictor carries stronger phylogenetic signal. Preliminary evidence from Chen et al. (2023, preprint) suggests that such mismatches can distort trait–trait estimates. In contrast, PVR's symmetrical framework avoids directional assumptions, enabling more balanced inference when causal directions are ambiguous or reciprocal.

4.3. Reassessing the SPV ≥ 10 Rule in the Context of PVR

The "SPV ≥ 10" rule, widely recommended in conventional regression to guard against overfitting and unstable inference (Austin et al., 2017; Babyak, 2004; Peduzzi et al., 1996), does not directly apply to PVR because eigenvectors are orthogonal rather than correlated predictors. Mechanically importing such heuristics into phylogenetic contexts risks misrepresenting model reliability. Our analyses indicate that PVR remains reliable with much lower SPV, with accuracy still acceptable when SPV falls to ~3. This tolerance affords greater flexibility, crucial for small datasets: with ≤19 species, SPV ≥ 10 precludes eigenvectors entirely, whereas a relaxed threshold of 3 allows inclusion of up to five.

Our analyses further suggest a practical guideline: regardless of the selection method, researchers should inspect the number of retained eigenvectors before incorporating them into regression models. For example, mAIC typically returns excessively large sets that risk overfitting, whereas mMorI may occasionally yield very few or even zero eigenvectors. Such checks are essential to ensure that PVR models remain both parsimonious and effective.

4.4. Broader implications: variable asymmetry beyond phylogenetic models

Although our focus is on phylogenetic comparative methods, similar issues arise in spatial analyses, where spatial autocorrelation must also be accounted for (Cottenie, 2005; Dale and Fortin, 2009; Diniz-Filho and Bini, 2005; He et al., 2003; Keitt et al., 2002; Legendre, 1993; Peres-Neto and Legendre, 2010). Preliminary tests show that the asymmetry introduced by variable designation—discussed for PVR—also affects spatial frameworks such as spatial eigenvector mapping, CAR, SAR, and trend-surface GAMs, with performance differing when dependent and independent variables are swapped (Table S7). By analogy, the union-based strategy we adopted for PVR may also apply to spatial analyses, potentially helping to preserve shared spatial signal while controlling autocorrelation.

In real datasets, multiple autocorrelation structures (e.g., spatial, phylogenetic, environmental) often coexist, further complicating model choice. As highlighted by Safi and Pettorelli (2010), balancing these components requires aligning methods with biological structure. Extending PVR and related approaches to flexibly integrate multiple forms of autocorrelation may therefore enhance model robustness in complex ecological scenarios.

CRediT authorship contribution statement

Z.-L. Chen: Writing – original draft, Visualization, Validation, Software, Methodology, Investigation, Formal analysis, Data curation. **D.-K. Niu**: Conceptualization, Writing – original draft, Writing – review & editing, Supervision, Resources, Funding acquisition.

Declaration of competing interest

The authors declare that they have no known competing financial interests or personal relationships that could have appeared to influence the work reported in this paper.

Acknowledgments

We are grateful to the reviewers of a previous submission for their constructive feedback, especially Prof. J.A.F. Diniz-Filho, who kindly signed his review, and an anonymous reviewer whose detailed suggestions helped refine our analysis. This work was supported by the National Natural Science Foundation of China (grant 31671321), with residual funds covering incidental research costs. Language polishing was assisted by ChatGPT-4o and subsequent versions; all edits were reviewed by the authors, who take full responsibility for the final content.

Appendix A. Supplementary data

Supplementary Information, including Text S1, Tables S1-S7, and Figures S1-S11, is submitted with this manuscript as online Supporting Information.

Data availability

The scripts used to generate the results in the main text—including phylogenetic tree construction, trait data simulation, regression model fitting, and statistical analysis—are provided in Main_code.zip. The relevant codes for evaluating spatial statistical methods are available in Spatial_methods.zip. In addition, we have developed an R package, ROBPVRU, which implements phylogenetic eigenvector regression with union operations on eigenvectors combined with robust estimators. All these materials and the data used to generate Fig. 1 and the supplementary figures, are freely accessible at https://github.com/zhenglinchen/PVR.

References

Adams, R., Cain, Z., Assis, R., DeGiorgio, M., 2024. Robust phylogenetic regression. Syst. Biol. 73, 140-157. https://doi.org/10.1093/sysbio/syad070

Austin, P.C., Allignol, A., Fine, J.P., 2017. The number of primary events per variable affects estimation of the subdistribution hazard competing risks model. Journal of Clinical Epidemiology 83, 75-84. https://doi.org/https://doi.org/10.1016/j.jclinepi.2016.11.017

Babyak, M.A., 2004. What you see may not be what you get: a brief, nontechnical introduction to overfitting in regression-type models. Psychosom. Med. 66, 411-421. https://doi.org/10.1097/01.psy.0000127692.23278.a9

Casson, R.J., Farmer, L.D., 2014. Understanding and checking the assumptions of linear regression: a primer for medical researchers. Clin. Exp. Ophthalmol. 42, 590-596. https://doi.org/https://doi.org/10.1111/ceo.12358

Chen, Z.-L., Guo, H.-J., Niu, D.-K., 2023. Dependent variable selection in phylogenetic generalized least squares regression analysis under Pagel's lambda model. bioRxiv, 2023.2005.2021.541623. https://doi.org/10.1101/2023.05.21.541623

Chen, Z.-L., Huang, R., Guo, H.-J., Niu, D.-K., 2025. Improving the robustness of phylogenetic independent contrasts: addressing abrupt evolutionary shifts with outlier- and distribution-guided correlation. bioRxiv, 2024.2006.2016.599156. https://doi.org/10.1101/2024.06.16.599156

Cheverud, J.M., Dow, M.M., Leutenegger, W., 1985. The quantitative assessment of phylogenetic constraints in comparative analyses: sexual dimorphism in body weight among primates. Evolution 39, 1335-1351. https://doi.org/10.1111/j.1558-5646.1985.tb05699.x

Cornwallis, C.K., Griffin, A.S., 2024. A guided tour of phylogenetic comparative methods for studying trait evolution. Annu. Rev. Ecol. Evol. Syst. 55, 181-204. https://doi.org/10.1146/annurev-ecolsys-102221-050754

Cottenie, K., 2005. Integrating environmental and spatial processes in ecological community dynamics. Ecol. Lett. 8, 1175-1182. https://doi.org/10.1111/j.1461-0248.2005.00820.x

Dale, M.R.T., Fortin, M.-J., 2009. Spatial autocorrelation and statistical tests: Some solutions. JABES 14, 188-206. https://doi.org/10.1198/jabes.2009.0012

Debastiani, V.J., Bastazini, V.A.G., Pillar, V.D., 2021. Using phylogenetic information to impute missing functional trait values in ecological databases. Ecol. Inform. 63, 101315. https://doi.org/10.1016/j.ecoinf.2021.101315

Dewar, A.E., Belcher, L.J., West, S.A., 2025. A phylogenetic approach to comparative genomics. Nat. Rev. Genet. 26, 395-405. https://doi.org/10.1038/s41576-024-00803-0

Diniz-Filho, J.A.F., Alves, D.M.C.C., Villalobos, F., Sakamoto, M., Brusatte, S.L., Bini, L.M., 2015. Phylogenetic eigenvectors and nonstationarity in the evolution of theropod dinosaur skulls. J. Evol. Biol. 28, 1410-1416. https://doi.org/10.1111/jeb.12660

Diniz-Filho, J.A.F., Bini, L.M., 2005. Modelling geographical patterns in species richness using eigenvector-based spatial filters. Glob. Ecol. Biogeogr. 14, 177-185. https://doi.org/10.1111/j.1466-822X.2005.00147.x

Diniz-Filho, J.A.F., Bini, L.M., Rangel, T.F., Morales-Castilla, I., Olalla-Tárraga, M.Á., Rodríguez, M.Á., Hawkins, B.A., 2012a. On the selection of phylogenetic eigenvectors for

ecological analyses. Ecography 35, 239-249. https://doi.org/10.1111/j.1600-0587.2011.06949.x

Diniz-Filho, J.A.F., Bini, M., Sakamoto, M., Brusatte, S., 2014. Phylogenetic eigenvector regression in paleobiology. Rev. Bras. Paleontol. 17, 107-122. https://doi.org/10.4072/rbp.2014.2.01

Diniz-Filho, J.A.F., Cianciaruso, M.V., Rangel, T.F., Bini, L.M., 2011. Eigenvector estimation of phylogenetic and functional diversity. Funct. Ecol. 25, 735-744. https://doi.org/10.1111/j.1365-2435.2011.01836.x

Diniz-Filho, J.A.F., de Sant'Ana, C.E.R., Bini, L.M., 1998. An eigenvector method for estimating phylogenetic inertia. Evolution 52, 1247-1262. https://doi.org/10.1111/j.1558-5646.1998.tb02006.x

Diniz-Filho, J.A.F., Jardim, L., Mondanaro, A., Raia, P., 2019. Multiple components of phylogenetic non-stationarity in the evolution of brain size in fossil Hominins. Evol. Biol. 46, 47-59. https://doi.org/10.1007/s11692-019-09471-z

Diniz-Filho, J.A.F., Nabout, J.C., 2009. Modeling body size evolution in Felidae under alternative phylogenetic hypotheses. Genet Mol Biol 32, 170-176. https://doi.org/10.1590/s1415-47572009005000004

Diniz-Filho, J.A.F., Rangel, T.F., Santos, T., Mauricio Bini, L., 2012b. Exploring patterns of interspecific variation in quantitative traits using sequential phylogenetic eigenvector regressions. Evolution 66, 1079-1090. https://doi.org/10.1111/j.1558-5646.2011.01499.x

Diniz-Filho, J.A.F., Tôrres, N.M., 2002. Phylogenetic comparative methods and the geographic range size – body size relationship in new world terrestrial carnivora. Evol. Ecol. 16, 351-367. https://doi.org/10.1023/A:1020210321776

Divíšek, J., Chytrý, M., Beckage, B., Gotelli, N.J., Lososová, Z., Pyšek, P., Richardson, D.M., Molofsky, J., 2018. Similarity of introduced plant species to native ones facilitates naturalization, but differences enhance invasion success. Nat. Commun. 9, 4631. https://doi.org/10.1038/s41467-018-06995-4

Felsenstein, J., 1985. Phylogenies and the comparative method. Amer. Natur. 125, 1-15. https://doi.org/10.1086/284325

Freckleton, R.P., Cooper, N., Jetz, W., 2011. Comparative methods as a statistical fix: the dangers of ignoring an evolutionary model. Amer. Natur. 178, E10-E17. https://doi.org/10.1086/660272

Gao, X., Dai, J., Tao, Z., Shahzad, K., Wang, H., 2023. Autumn phenology of tree species in China is associated more with climate than with spring phenology and phylogeny. Front. Plant Sci. 14, 1040758. https://doi.org/10.3389/fpls.2023.1040758

Garamszegi, L.Z., 2014. Modern Phylogenetic Comparative Methods and Their Application in Evolutionary Biology: Concepts and Practice. Springer, Berlin. https://doi.org/10.1007/978-3-662-43550-2

Gervini, D., Yohai, V.J., 2002. A class of robust and fully efficient regression estimators. Ann. Statist. 30, 583-616. https://doi.org/10.1214/aos/1021379866

Gouveia, S.F., Hortal, J., Cassemiro, F.A.S., Rangel, T.F., Diniz-Filho, J.A.F., 2013. Nonstationary effects of productivity, seasonality, and historical climate changes on global amphibian diversity. Ecography 36, 104-113. https://doi.org/10.1111/j.1600-0587.2012.07553.x

Grafen, A., 1989. The phylogenetic regression. Philos. Trans. R. Soc. Lond. B Biol. Sci. 326, 119-157. https://doi.org/10.1098/rstb.1989.0106

He, F., Zhou, J., Zhu, H., 2003. Autologistic regression model for the distribution of vegetation. JABES 8, 205-222. https://doi.org/10.1198/1085711031508

Huber, P.J., 1964. Robust estimation of a location parameter. Ann. Math. Statist. 35, 73-101.

Jarantow, S.W., Pisors, E.D., Chiu, M.L., 2023. Introduction to the use of linear and nonlinear regression analysis in quantitative biological assays. Curr. Protoc. 3, e801. https://doi.org/10.1002/cpz1.801

Keitt, T.H., Bjørnstad, O.N., Dixon, P.M., Citron-Pousty, S., 2002. Accounting for spatial pattern when modeling organism-environment interactions. Ecography 25, 616-625. https://doi.org/10.1034/j.1600-0587.2002.250509.x

Kühn, I., Nobis, M.P., Durka, W., 2009. Combining spatial and phylogenetic eigenvector filtering in trait analysis. Glob. Ecol. Biogeogr. 18, 745-758. https://doi.org/https://doi.org/10.1111/j.1466-8238.2009.00481.x

Lanuza, J.B., Rader, R., Stavert, J., Kendall, L.K., Saunders, M.E., Bartomeus, I., 2023. Covariation among reproductive traits in flowering plants shapes their interactions with pollinators. Funct. Ecol. 37, 2072-2084. https://doi.org/10.1111/1365-2435.14340

Laurin, M., 2010. Assessment of the relative merits of a few methods to detect evolutionary trends. Syst. Biol. 59, 689-704. https://doi.org/10.1093/sysbio/syq059

Legendre, P., 1993. Spatial autocorrelation: trouble or new paradigm? Ecology 74, 1659-1673. https://doi.org/10.2307/1939924

LeRoy, C.J., Hipp, A.L., Lueders, K., Follstad Shah, J.J., Kominoski, J.S., Ardón, M., Dodds, W.K., Gessner, M.O., Griffiths, N.A., Lecerf, A., Manning, D.W.P., Sinsabaugh, R.L., Webster, J.R., 2020. Plant phylogenetic history explains in-stream decomposition at a global scale. J Ecol 108, 17-35. https://doi.org/10.1111/1365-2745.13262

Maynard, D.S., Bialic-Murphy, L., Zohner, C.M., Averill, C., van den Hoogen, J., Ma, H., Mo, L., Smith, G.R., Acosta, A.T.R., Aubin, I., Berenguer, E., Boonman, C.C.F., Catford, J.A., Cerabolini, B.E.L., Dias, A.S., González-Melo, A., Hietz, P., Lusk, C.H., Mori, A.S., Niinemets, Ü., Pillar, V.D., Pinho, B.X., Rosell, J.A., Schurr, F.M., Sheremetev, S.N., da Silva, A.C., Sosinski, Ê., van Bodegom, P.M., Weiher, E., Bönisch, G., Kattge, J., Crowther, T.W., 2022. Global relationships in tree functional traits. Nat. Commun. 13, 3185. https://doi.org/10.1038/s41467-022-30888-2

McArdle, B.H., 1988. The structural relationship: regression in biology. Can. J. Zool. 66, 2329-2339. https://doi.org/10.1139/z88-348

Osborne, J.W., Waters, E., 2002. Four assumptions of multiple regression that researchers should always test. Pract. Assess. Res. Eval. 8, 2. https://doi.org/10.7275/r222-hv23

Paradis, E., Schliep, K., 2019. ape 5.0: an environment for modern phylogenetics and evolutionary analyses in R. Bioinformatics 35, 526-528. https://doi.org/10.1093/bioinformatics/bty633

Peduzzi, P., Concato, J., Kemper, E., Holford, T.R., Feinstein, A.R., 1996. A simulation study of the number of events per variable in logistic regression analysis. Journal of Clinical Epidemiology 49, 1373-1379. https://doi.org/https://doi.org/10.1016/S0895-4356(96)00236-3

Pennell, M.W., Harmon, L.J., 2013. An integrative view of phylogenetic comparative methods: connections to population genetics, community ecology, and paleobiology. Ann NY Acad Sci 1289, 90-105. https://doi.org/https://doi.org/10.1111/nyas.12157

Penone, C., Davidson, A.D., Shoemaker, K.T., Di Marco, M., Rondinini, C., Brooks, T.M., Young, B.E., Graham, C.H., Costa, G.C., 2014. Imputation of missing data in life-history trait datasets: which approach performs the best? Methods Ecol. Evol. 5, 961-970. https://doi.org/10.1111/2041-210X.12232

Peres-Neto, P.R., Legendre, P., 2010. Estimating and controlling for spatial structure in the study of ecological communities. Glob. Ecol. Biogeogr. 19, 174-184. https://doi.org/10.1111/j.1466-8238.2009.00506.x

Peres-Neto, P.R., Leibold, M.A., Dray, S., 2012. Assessing the effects of spatial contingency and environmental filtering on metacommunity phylogenetics. Ecology 93, S14-S30. https://doi.org/10.1890/11-0494.1

Phillips, R.F., 2002. Least absolute deviations estimation via the EM algorithm. Statistics and Computing 12, 281-285. https://doi.org/10.1023/A:1020759012226

Revell, L.J., 2010. Phylogenetic signal and linear regression on species data. Methods Ecol. Evol. 1, 319-329. https://doi.org/10.1111/j.2041-210X.2010.00044.x

Revell, L.J., 2024. phytools 2.0: an updated R ecosystem for phylogenetic comparative methods (and other things). PeerJ 12, e16505. https://doi.org/10.7717/peerj.16505

Safi, K., Pettorelli, N., 2010. Phylogenetic, spatial and environmental components of extinction risk in carnivores. Glob. Ecol. Biogeogr. 19, 352-362. https://doi.org/10.1111/j.1466-8238.2010.00523.x

Slater, G.J., Pennell, M.W., 2014. Robust regression and posterior predictive simulation increase power to detect early bursts of trait evolution. Syst. Biol. 63, 293-308. https://doi.org/10.1093/sysbio/syt066

Venables, W.N., Ripley, B.D., 2002. Modern Applied Statistics with S, 4th ed. Springer.

Wang, Z.H., Jiang, Y., Deane, D.C., He, F.L., Shu, W.S., Liu, Y., 2019. Effects of host phylogeny, habitat and spatial proximity on host specificity and diversity of pathogenic and mycorrhizal fungi in a subtropical forest. New Phytol. 223, 462-474. https://doi.org/10.1111/nph.15786

Westoby, M., Yates, L., Holland, B., Halliwell, B., 2023. Phylogenetically conservative trait correlation: Quantification and interpretation. J Ecol 111, 2105-2117. https://doi.org/10.1111/1365-2745.14150

Yu, C., Yao, W., 2017. Robust linear regression: A review and comparison. Commun. Stat. Simul. Comput. 46, 6261-6282. https://doi.org/10.1080/03610918.2016.1202271